RSC Advances

PAPER

View Article Online
View Journal | View Issue

Cite this: *RSC Adv.*, 2019, **9**, 14657

Effect of polymer molecular weight on J51 based organic solar cells

Yangqian Zhang, Xiangfei Xu, Jiaorong Lu and Shiming Zhang *

Received 15th March 2019
Accepted 2nd May 2019

DOI: 10.1039/c9ra02022e

rsc.li/rsc-advances

Very recently, organic solar cells (OSCs) have achieved outstanding scientific results with a power conversion efficiency (PCE) of over 16%. However, it is rarely reported on how molecular weight (M_n) of polymer donors affects the solar cell performances. In this work, the wide bandgap polymer donor J51 with different M_n from 8 to 36 kDa were synthesized and used for fabrication of J51:$PC_{71}BM$ devices. It was found that the PCEs were gradually on the increase with the increased molecular weight of J51 donor. This work demonstrated the relationship between devices performance and polymer molecular weight, which enriched the OSCs research content. It provides valuable reference information that optimal molecular weight of polymer donors should be limited in what is considered the applicable range.

Introduction

Organic solar cells (OSCs) are getting more and more attention because of the increasingly serious environmental pollution of the past decades. Compared to inorganic Si solar cells, OSCs possess outstanding advantages such as low-cost, lightweight, solution process-ability and fabrication on large/flexible substrates.[1–3] The typical OSCs' bulk heterojunction (BHJ) structure has been considered as the most perspective structure which is studied and used extensively by far.[4] The BHJ solar cells consist of conjugated polymers as donors and fullerene/non-fullerene derivatives as acceptors. At present, P2F-EHp:BTPTT-4F-based single junction OSCs displayed a PCE record of over 16% attributed to a fine phase-separated morphology, which is very close to commercialized inorganic solar cells.[5] The rapid developments of OSCs mainly depend on optimization of donor and acceptor materials' pair, device structure and interfacial engineering.[6–8] In brief, continuous evolution of donor and acceptor materials have contributed for the advance of BHJ solar cells. The performance of BHJ devices is deeply affected by light absorption, HOMO and LUMO energy levels, solubility and morphology.[9–12] Fullerene acceptors such as $PC_{61}BM$ and $PC_{71}BM$ played an important role in the development of OSCs.[13–17] $PC_{61}BM$ and $PC_{71}BM$ have excellent charge mobility, deep HOMO/LUMO levels and isotropic properties.[18–20] For a long time, researchers sought for all kinds of polymer donors to match with fullerene acceptors, especially low band gap conjugated polymers.[21–24] Molecular weight is one of the most important parameter for polymer donors because molecular weight directly influences optical-electricity property, solubility and the morphology of the active layer.[25–31] Relatively little efforts have been made to reveal how polymer molecular weight affects the device performance in OSCs, as it is difficult to control the polymer molecular weight well during the synthesis. With the increase of PBTIBDTT-S' M_n from 12 to 38 kDa, the PCEs of PBTIBDTT-S:$PC_{71}BM$ devices gradually increased due to the large improvement in J_{sc} and slight enhancement in FF.[32] The performance of PTB7-Th:PNDITF4T improved successfully with enhanced PNDITF4T M_n from 22 to 87 kDa while drastically reduced with M_n over 167 kDa. The too high M_n of polymer acceptor showed liquid–liquid phase separation leading to augmented exciton recombination.[33] Hence, it is possible to infer that the performance of BHJ devices does not always improve with increasing molecular weight of donor or acceptor. The famous D–A type copolymer PBDT–FBTA (J51) was first reported by Li's group.[34] The OSCs based on J51:$PC_{71}BM$ blends with 5% DIO obtained a maximum PCE of 6.0%. In this work, we synthesized a series of polymer J51 with different M_n of 8, 16, 21 and 36 kDa. The relationship between polymer molecular weight and performance of OSC devices was studied by preparing OSCs with J51 as donor and $PC_{71}BM$ as acceptor. It was found that, when the molecular weight of polymer J51 was increased, the open circuit voltage (V_{OC}) of corresponding device slightly increased, while the short circuit current (J_{SC}) and fill factor (FF) were gradually enhanced. The gradually enhanced PCE is attributed to the enhanced light harvest ability, reduced carrier recombination and superior morphology of active layer.[34,35] Our work revealed the dependence of device performance on polymer molecular weight in polymer OSCs and demonstrated the importance of suitable M_n in achieving high performance fullerene OSCs, which would benefit for the breakthrough in PCEs for fullerene OSCs (Fig. 1).

Key Laboratory of Flexible Electronics (KLOFE) & Institute of Advanced Materials (IAM), Jiangsu National Synergetic Innovation Center for Advanced Materials (SICAM), Nanjing Tech University, 30 South Puzhu Road, Nanjing 211816, Jiangsu, P. R. China. E-mail: iamsmzhang@njtech.edu.cn

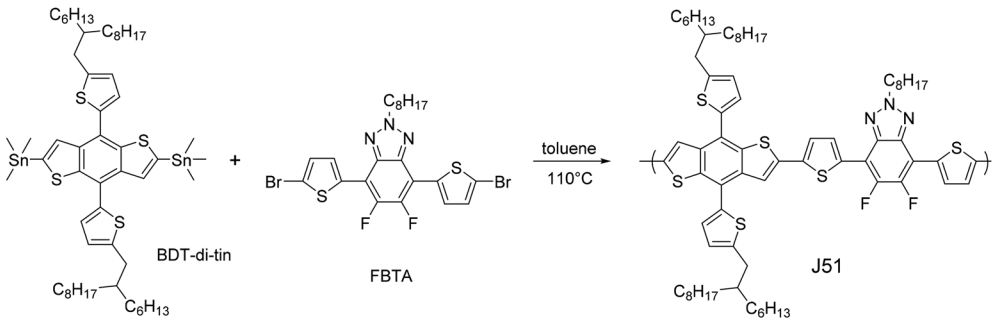

Fig. 1 The synthesis of four polymer J51 with different M_n.

Results and discussion

All OSCs based on J51:$PC_{71}BM$ were fabricated in an inverted architecture using different molecular weight of J51 (in the range between 8 kDa and 36 kDa). Details of device fabrication are provided in the Experimental section. Here, polymer J51 with different molecular weight from 8 to 36 kDa is further studied and the absorption spectra of single J51 solutions in chloroform are shown in Fig. 2a. The J51 polymer is known as a wide band polymer. When molecular weight increased, J51 polymers showed distinctly red-shift in Fig. 2a. It can be observed that the peaks of absorption was red-shifted from 529 nm of J51-8kDa to 601 nm of J51-36kDa. The gradually improved absorption of J51 with a molecular weight range of M_n from 8 to 36 kDa indicated the enhanced molecular π–π stacking.[36–38] The gradually enhanced absorption coefficient contributes to the higher J_{SC} furtherly.[39] The absorption spectra of single J51 films are shown in Fig. 2b. It was found that the peaks of absorption was red-shifted from 442 nm of J51-8kDa to 521 nm of J51-36kDa. Compared to the absorption in solution, the peaks of absorption was relatively blue-shifted, which may result from their unique H-aggregation-induced interchain packing in the solid state.

The current density–voltage (*J*–*V*) curves of J51:$PC_{71}BM$ blends under illumination are shown in Fig. 3 and the photovoltaic performance parameters are summarized in Table 1. The best performance was obtained when used J51-36kDa as donor with a V_{OC} of 753 mV, a J_{SC} of 12.18 mA cm^{-2}, a FF of 65.06%, and a PCE of 5.97%. This excellent performance is mainly attributable to the reasonably high J_{SC} and FF values together. Based on the results, the device PCE performance significantly improves with increasing the molecular weight of J51 from 1.56% (J51-8kDa) to 5.97% (J51-36kDa) due to increased photocurrent generation. By comparing the device performance parameters, it is found that the V_{OC} value slightly increases from 720 mV (J51-8kDa) to 753 mV (J51-36kDa), while the J_{SC} and FF prominently increase from 5.42 to 12.18 mA cm^{-2} and 39.89% to 65.06%, respectively, because of the higher molar mass fractions, the higher charge mobility.[40,41]

The surface morphology of optimal J51:$PC_{71}BM$ blends on ZnO-coated ITO was examined *via* atomic force microscopy (AFM) and measured in tapping mode (as shown in Fig. 4). As for J51-8kDa and J51-16kDa blend films, relatively rough surfaces were observed with similar RMSs of 2.07 and 1.31 nm, leading to poor device performances, respectively. For J51-21kDa blend film, good smooth surface was exhibited with small RMS of 1.22 nm. While for the blend film based on J51-36kDa, ultra-fine and homogeneous nanocrystals were surveyed with the minimum RMS of 1.15 nm, which was attributed to the highest crystallinity of active layer among these four polymers with different molecular weight. So the roughness of blend thin films was decreased and domain size was reduced when the polymer's molecular weight was improved. The smaller the roughness for blend films, the higher the efficiency of blend devices.

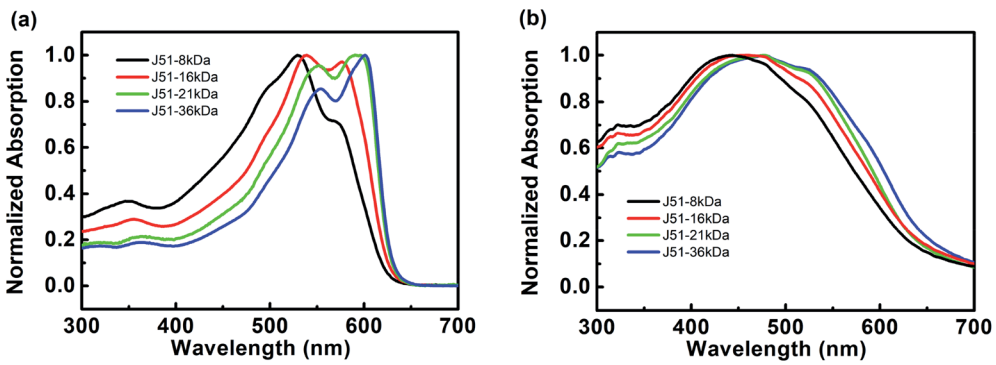

Fig. 2 The absorption spectra of the pure J51 with different M_n both in (a) chloroform solution and (b) film state.

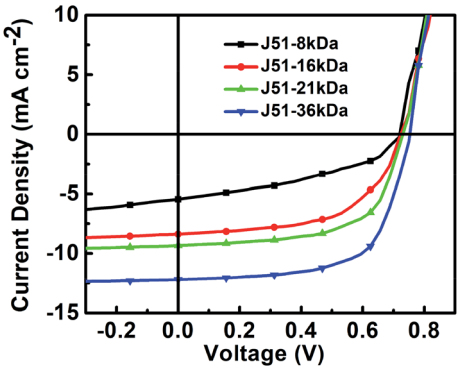

Fig. 3 J–V curves of J51:$PC_{71}BM$ solar cells under illumination.

Table 1 Photovoltaic parameters of OSCs based on J51:$PC_{71}BM$

Polymer	M_n [kDa]	V_{OC} [mV]	J_{SC} [mA cm^{-2}]	FF [%]	PCE [%]
J51-8kDa	8	720	5.42	39.89	1.56
J51-16kDa	16	724	8.35	58.20	3.52
J51-21kDa	21	730	9.31	61.85	4.20
J51-36kDa	36	753	12.18	65.06	5.97

Experimental section

Chemicals and materials

We strictly controlled both molar ratio of BDT-di-tin and FBTA, as well as reaction time to synthesize four polymer J51 with different M_n.

All J51 polymers (J51-8kDa, J51-16kDa, J51-21kDa and J51-36kDa) were synthesized *via* Stille coupling reaction as showed in synthesis part. ITO-coated glass substrates with specification of 12 × 12 mm^2 were used for devices. Zinc acetate dihydrate ($Zn(CH_3COO)_2 \cdot 2H_2O$, ≥99.5%), 2-methoxyethanol (99.8%, anhydrous) and molybdenum(VI) oxide (99.98%, trace metals basis) were obtained from Sigma-Aldrich. Ethanolamine (98%) was purchased from Sigma-Aldrich. Silver (99.99%) was obtained from Zhongnuo. Chloroform was obtained by distillations with calcium chloride to dry in advance. Building block 4,7-bis(5-bromothiophen-2-yl)-2-(2-butyloctyl)-5,6-difluoro-2*H*-benzo[d][1,2,3]triazole (FBTA) and BDT di-tin monomer were synthesized according to literature. Except for J51 with different M_ns and chloroform, all the other chemicals were used as received without further purification.

Synthesis of J51 polymers

Synthesis of J51-16kDa: compound FBTA (117.8 mg, 0.2 mmol) and BDT di-tin (214.5 mg, 0.19 mmol) were added into a 25 mL Shrek tube with 10 mL of anhydrous toluene, after nitrogen bubbled for 0.5 h, $Pd(PPh_3)_4$ (11.6 mg, 0.01 mmol) was added under the oxygen-free environment, then the reaction mixture was heated to 110 °C and stirred for 72 h under the nitrogen atmosphere, and then an excess amount of trimethyl(thienyl)tin and bromobenzene were added to end-cap the bromo and trimethylstannyl groups, respectively. Stopped stirring and cooled down to room temperature, the reaction mixture was dropped into 200 mL of methanol solution and stirred for 1 h, then filtered. The precipitate was collected and purified by the Soxhlet extraction with methanol and acetone, followed by chloroform for 24 h, respectively. The chloroform fraction was concentrated under reduced pressure and then added into methanol solution dropwised. The precipitate was collected and dried in vacuum to yield a solid (153.4 mg, 65.5%). GPC (DCB at 120 °C): M_n = 16 kg mol^{-1}, M_w = 22 kg mol^{-1}, PDI = 1.38.

The synthesis of J51-8kDa followed the same procedure for J51-16kDa except the reactants were stirred under reflex for 20 hours with yield ratio of 31.5%. GPC (DCB at 120 °C): M_n = 8 kg mol^{-1}, M_w = 13 kg mol^{-1}, PDI = 1.63.

The synthesis of J51-36kDa followed the same procedure for J51-16kDa except the ratio of FBTA : BDT di-tin equals exactly to 1, the yield ratio is about 86.7%. GPC (DCB at 120 °C): M_n = 36 kg mol^{-1}, M_w = 48 kg mol^{-1}, PDI = 1.33.

The synthesis of J51-21kDa followed the same procedure for J51-36kDa except the reactants were stirred under reflex for 48 hours with yield ratio of 53.8%. GPC (DCB at 120 °C): M_n = 21 kg mol^{-1}, M_w = 27 kg mol^{-1}, PDI = 1.29.

Device fabrication and characterization

The OSCs were fabricated in an inverted architecture of glass/ITO/ZnO (40 nm)/active layer/MoO_3 (10 nm)/Ag (90 nm). Glass substrates were pre-patterned with ITO and cleaned by sonication in detergent, deionized water, acetone, and isopropanol before ozone plasma treatment (10 min). A layer of ZnO (from solution of 100 mg $2H_2O \cdot Zn(OAc)_2$ in 28 μl ethanolamine and

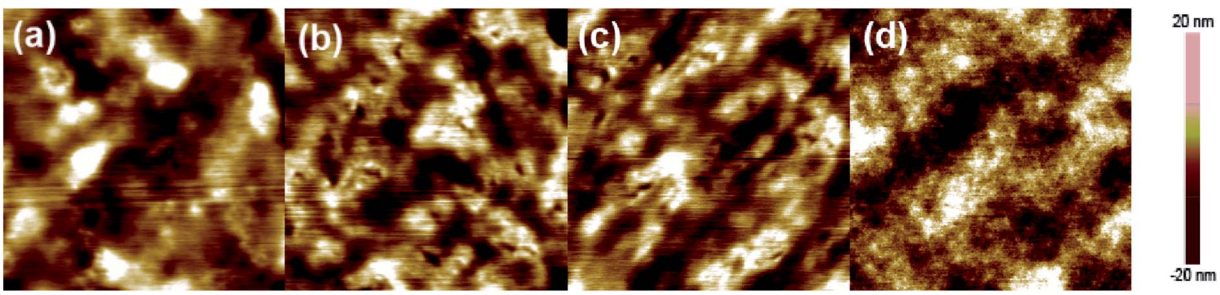

Fig. 4 AFM topography images (a–d) of J51:$PC_{71}BM$ blend thin films with J51-8kDa (a), J51-16kDa (b), J51-21kDa (c), and J51-36kDa (d) (image size: 5 × 5 μm^2).

1 mL 2-methoxyethanol), was obtained by spin-coating onto the ITO substrate at 4000 rpm for 40 s, followed by annealing at 200 °C for 60 min in air. The active layer was formed by spin-coating chloroform solution, containing a blend of J51 with $PC_{71}BM$ in 1 : 1 weight ratios. 1,8-Diiodooctane (DIO) with 5% volume ratio was added to the chloroform solutions and stirred at 40 °C overnight before use. Finally, a MoO_3/Ag anode electrode was deposited in vacuum onto the active layer through a shadow mask at a pressure of *ca.* 5×10^{-4} Pa. The active area of the device was estimated at 4 mm^2. The *J–V* characteristics were measured using a Keithley 2400 source meter under AM1.5G (100 mW cm^{-2}) irradiation with an Oriel Instruments Xenon lamp calibrated to a Si reference cell to correct for spectral mismatch.

Conclusions

This work demonstrated an obviously influence of the molecular weight of J51 on the photovoltaic performance of J51:$PC_{71}BM$ based organic solar cells. The PCEs gradually increased from 1.56% to 5.97% with the molecular weight changed from 8 to 36 kDa due to the substantial increment in J_{SC} and FF, while the V_{OC} remained very similar to each other. The optical absorption, morphologies and photovoltaic properties were systematically investigated. These test results enhance the importance of the molecular weight of polymers as an important factor for high performance OSCs. Hence, except for the chemical structure design of the polymer donors or acceptors, the optimal molecular weight fraction should also be considered in order to promote further development of polymer-based organic solar cells.

Conflicts of interest

There are no conflicts to declare.

Acknowledgements

The authors acknowledge financial support from the National Natural Science Foundation of China (Grant No. 61574077) and the National Key R&D Program of Strategic Advanced Electronic Materials" (No. 2016YFB0401100).

References

1 S. H. Park, A. Roy, S. Beaupré, S. Cho, N. Coates, J. S. Moon, D. Moses, M. Leclerc, K. Lee and A. J. Heeger, *Nat. Photonics*, 2009, **3**, 297–303.
2 K. Mazzio and C. Luscombe, *Chem. Soc. Rev.*, 2015, **44**, 78–90.
3 H. Lin, S. Chen, Z. Li, J. Y. L. Lai, G. Yang, T. McAfee, K. Jiang, Y. Li, Y. Liu, H. Hu, J. Zhao, W. Ma, H. Ade and H. Yan, *Adv. Mater.*, 2015, **27**, 7299–7304.
4 G. Yu, J. Gao, J. C. Hummelen, F. Wudi and A. J. Heeger, *Science*, 1995, **270**, 1789–1791.
5 B. Fan, D. Zhang, M. Li, W. Zhong, Z. Zeng, L. Ying, F. Huang and Y. Cao, *Sci. China: Chem.*, 2019, **62**, DOI: 10.1007/s11426-019-9457-5.
6 Y. Li, Y. Xu, F. Yang, X. Jiang, C. Li, S. You and W. Li, *Chin. Chem. Lett.*, 2019, **30**, 222–224.
7 S. Zhou, G. Feng, D. Xia, C. Li, Y. Wu and W. Li, *Acta Phys. –Chim. Sin.*, 2018, **34**, 344–347.
8 H. Li, Z. Xiao, L. Ding and J. Wang, *Sci. Bull.*, 2018, **63**, 340–342.
9 F. Yang, C. Li, G. Feng, X. Jiang, A. Zhang and W. Li, *Chin. J. Polym. Sci.*, 2017, **35**, 239–248.
10 J. Yuan, Y. Zhang, L. Zhou, G. Zhang, H. Yip, T. Lau, X. Lu, C. Zhu, H. Peng, P. Johnson, M. Leclerc, Y. Cao, J. Ulanski, Y. Li and Y. Zou, *Joule*, 2019, **3**, 1–12.
11 R. Arai, S. Furukawa, Y. Hidaka, H. Komiyama and T. Yasuda, *ACS Appl. Mater. Interfaces*, 2019, **11**, 9259–9264.
12 L. Meng, Y. Zhang, X. Wan, C. Li, X. Zhang, Y. Wang, X. Ke, Z. Xiao, L. Ding, R. Xi, H. Yip, Y. Cao and Y. Chen, *Science*, 2018, **361**, 1094–1098.
13 B. C. Thompson and J. M. J. Fréchet, *Angew. Chem., Int. Ed.*, 2008, **47**, 58–77.
14 Z. He, C. Zhong, S. Su, M. Xu, H. Wu and Y. Cao, *Nat. Photonics*, 2012, **6**, 591–595.
15 Z. Li, D. Yang, X. Zhao, T. Zhang, J. Zhang and X. Yang, *Adv. Funct. Mater.*, 2018, **28**, 1705257.
16 V. Cuesta, M. Vartanian, P. Malhotra, S. Biswas, P. Cruz, G. D. Sharma and F. Langa, *J. Mater. Chem. A*, 2019, **7**, 958–964.
17 T. Zhu, D. Liu, K. Zhang, Y. Li, Z. Liu, X. Gao, X. Bao, M. Sun and R. Yang, *J. Mater. Chem. A*, 2018, **6**, 948–956.
18 F. B. Kooistra, J. Knol, F. Kastenberg, L. M. Popescu, W. J. H. Verhees, J. M. Kroon and J. C. Hummelen, *Org. Lett.*, 2007, **9**, 551–554.
19 L. Zheng, Q. Zhou, X. Deng, M. Yuan, G. Yu and Y. Cao, *J. Phys. Chem. B*, 2004, **108**, 11921–11926.
20 G. Dennler, M. C. Scharber and C. J. Brabec, *Adv. Mater.*, 2009, **21**, 1323–1338.
21 Y. Li, *Acc. Chem. Res.*, 2012, **45**, 723–733.
22 B. C. Thompson and J. M. J. Fréchet, *Angew. Chem., Int. Ed.*, 2008, **47**, 58–77.
23 J. Chen and Y. Cao, *Acc. Chem. Res.*, 2009, **42**, 1709–1718.
24 Y. Cai, L. Huo and Y. Sun, *Adv. Mater.*, 2017, **29**, 1605437.
25 S. Goker, S. O. Hacioglu, G. Hizalan, E. Aktas, A. Cirpan and L. Toppare, *Macromol. Chem. Phys.*, 2017, **218**, 1600544.
26 Z. Li, D. Yang, T. Zhang, J. Zhang, X. Zhao and X. Yang, *Small*, 2018, **14**, 1704491.
27 N. Zhou, A. S. Dudnik, T. Li, E. F. Manley, T. J. Aldrich, P. Guo, H. Liao, Z. Chen, L. Chen, R. Chang, A. Facchetti, M. Olvera De La Cruz and T. J. Marks, *J. Am. Chem. Soc.*, 2016, **138**, 1240–1251.
28 W. Ma, G. Yang, K. Jiang, J. H. Carpenter, Y. Wu, X. Meng, T. McAfee, J. Zhao, C. Zhu, C. Wang, H. Ade and H. Yan, *Adv. Energy Mater.*, 2015, **5**, 1501400.
29 T. Chu, J. Lu, S. Beaupré, Y. Zhang, J. Pouliot, J. Zhou, A. Najari, M. Leclerc and Y. Tao, *Adv. Funct. Mater.*, 2012, **22**, 2345–2351.
30 M. Tong, S. Cho, J. T. Rogers, K. Schmidt, B. B. Y. Hsu, D. Moses, R. C. Coffin, E. J. Kramer, G. C. Bazan and A. J. Heeger, *Adv. Funct. Mater.*, 2010, **20**, 3959–3965.

31 W. Li, L. Yang, J. R. Tumbleston, L. Yan, H. Ade and W. You, *Adv. Mater.*, 2014, **26**, 4456–4462.
32 Z. Li, D. Yang, X. Zhao, T. Zhang, J. Zhang and X. Yang, *Adv. Funct. Mater.*, 2018, 1705257.
33 K. D. Deshmukh, R. Matsidik, S. K. K. Prasad, L. A. Connal, A. C. Y. Liu, E. Gann, L. Thomsen, J. M. Hodgkiss, M. Sommer and C. R. McNeill, *Adv. Funct. Mater.*, 2018, **28**, 1707185.
34 J. Min, Z. Zhang, S. Zhang and Y. Li, *Chem. Mater.*, 2012, **24**, 3247–3254.
35 L. Gao, Z. Zhang, L. Xue, J. Min, J. Zhang, Z. Wei and Y. Li, *Adv. Mater.*, 2016, **28**, 1884–1890.
36 H. Bin, L. Gao, Z. Zhang, Y. Yang, Y. Zhang, C. Zhang, S. Chen, L. Xue, C. Yang, M. Xiao and Y. Li, *Nat. Commun.*, 2016, **7**, 13651.
37 R. J. Kline, M. D. McGehee, E. N. Kadnikova, J. Liu and J. M. J. Fréchet, *Adv. Mater.*, 2003, **15**, 1519–1522.
38 R. Noriega, J. Rivnay, K. Vandewal, F. P. V. Koch, N. Stingelin, P. Smith, M. F. Toney and A. Salleo, *Nat. Mater.*, 2013, **12**, 1038–1044.
39 D. Qian, L. Ye, M. Zhang, Y. Liang, L. Li, Y. Huang, X. Guo, S. Zhang, Z. A. Tan and J. Hou, *Macromolecules*, 2012, **45**, 9611–9617.
40 W. Li, L. Yan, H. Zhou and W. You, *Chem. Mater.*, 2015, **27**, 6470–6476.
41 Z. Li, D. Yang, T. Zhang, J. Zhang, X. Zhao and X. Yang, *Small*, 2018, **14**, 1704491.